Temporal and spatial analysis of SST and thermal fronts in the North East Asia Seas using NOAA/AVHRR data

Hong-Joo Yoon

Department of Satellite Information Sciences, Pukyong National University, Busan, Korea
E-mail: yoonhj@pknu.ac.kr

ABSTRACT : NOAA/AVHRR data were used to analyze sea surface temperatures (SSTs) and thermal fronts (TFs) in the Korean seas. Temporal and spatial analyses were based on data from 1993 to 2000. Harmonic analysis revealed mean SST distributions of 10~25°C. Annual amplitudes and phases were 4~11°C and 210~240°, respectively. Inverse distributions of annual amplitudes and phases were found for the study seas, with the exception of the East China Sea, which is affected by the Kuroshio Current. Areas with high amplitudes (large variations in SSTs) showed "low phases" (early maximum SST); areas with low amplitudes (small variations in SSTs) had "high phases" (late maximum SST). Empirical orthogonal function (EOF) analyses of SSTs revealed a first-mode variance of 97.6%. Annually, greater SST variations occurred closer to the continent. Temporal components of the second mode showed higher values in 1993, 1994, and 1995. These phenomena seemed to the effect of El Niño. The Sobel edge detection method (SEDM) delineated four fronts: the Subpolar Front (SPF) separating the northern and southern parts of the East Sea; the Kuroshio Front (KF) in the East China Sea, the South Sea Coastal Front (SSCF) in the South Sea, and a tidal front (TDF) in the West Sea. Thermal fronts generally occurred over steep bathymetric slopes. Annual amplitudes and phases were bounded within these frontal areas. EOF analysis of SST gradient values revealed the temporal and spatial variations in the TFs. The SPF and SSCF were most intense in March and October; the KF was most significant in March and May.

Keywords: SST, Thermal Fronts, Harmonic Analysis, Sobel Edge Detection Method, EOF Analysis

1. INTRODUCTION

SSTs provide important quantitative measures of thermal features, such as oceanic fronts. Ocean fronts occur where two water masses with different properties meet and mix. The formation processes, shapes, and locations of ocean fronts vary. Ocean fronts are associated with, or occur near, current jets, enhanced variability, strong isopycnal and diapycnal mixing, water mass boundaries, biological ecozones and bioproductivity maxima, acoustical wave guides, marginal ice zones, and atmospheric boundary layer fronts (Berkin, 2002). Many researchers have used satellite data to study ocean fronts. Simpson, 1990, Cayula and Cornillon, 1995 and Shaw and Vennel, 2000 developed methods to extract ocean fronts and Deacon, 1982, Mavor and Bisagni, 2001, Wang *et. al.*, 2001 and Miller, 2004 analyzed variations and characteristics of ocean fronts. Ocean fronts in the Korean seas have been studied separately about the East, West and South seas using in-situ observations (Choi *et. al.*, 1993; Kim, 1998; Park *et. al.*, 1998; Yang *et. al.*, 1998; Lee *et. al.*, 2003).

This study constructed SSTs data and analyzed long term SSTs variations by applying time-series analysis methods and specially is aimed for extractions and classifications of thermal fronts (TFs) and examinations of their temporal and spatial variations using Advanced Very High Resolution Radiometer (AVHRR) data from the National Oceanic and Atmospheric Administration's (NOAA) series of polar-orbiting environmental satellites.

2. DATA AND METHODS

2.1 Data and study area

The AVHRR multi-channel sea surface temperature (MCSST) dataset, which contains weekly SST values, is derived by using McClain *et. al.*, 1985 method and is available in 19 × 19-km grids for the entire globe. A weekly period consists of 8 days so as to give a 1-day overlap between consecutive weekly files. We used archived MCSST data for 8 years, 1993~2000 and data containing mask values for areas of no data, sea ice, and land were provided by the Jet Propulsion Laboratory, Physical Oceanography Distributed Active Archive Center (JPL PO.DAAC; NASA/NOAA,1998). The MCSST dataset was chosen over the newer Pathfinder SST dataset because the MCSST can give more complete and continuous temporal coverage for the study period. The study area was 25°~45°N, 117°~142°E (Fig. 1). This area covers the West Sea, the East China Sea, the South Sea, and the East Sea, all of which influence the Korean seas.

SST data were validated using serial oceanographic data from the National Fisheries Research and Development Institute (NFRDI, Korea) (Fig. 2). Serial oceanographic data (SOD) from three stations in the West Sea (WS), South Sea (SS), and East Sea (ES) were compared with the most adjacent SST pixels. The correlation coefficients were high, above 0.8.

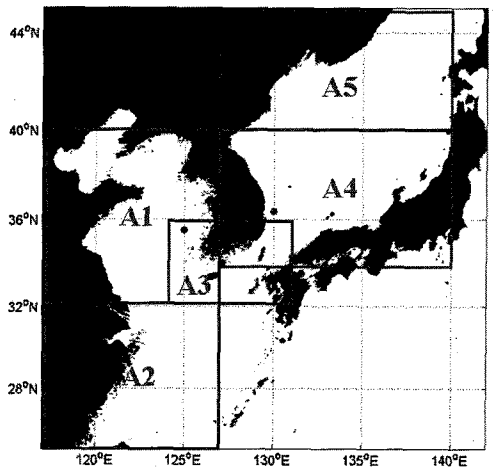

Fig. 1. Study Area (• : serial oceanographic data stations).

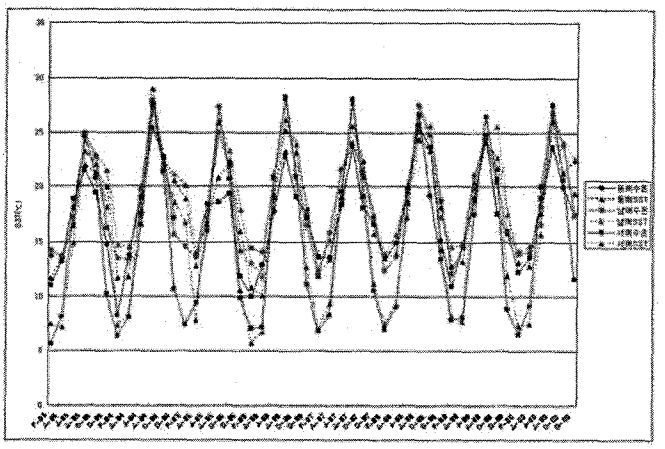

Fig. 2. Validation between Serial Oceanographic Data(SOD) and Satellite MCSST.

2.2 Methods

2.2.1 Harmonic Analysis

Harmonic analysis provided spatial distributions and seasonal SST variations in the Korean seas. The harmonic analysis equation is generally written as (Choi *et. al.*, 2000).

$$T(t) = \overline{T} + A_1 \cos(\omega_1 t - p_1) + A_2 \cos(\omega_2 t - p_2)$$

2.2.2 Sobel edge detection method (SEDM)

Sobel filtering can detect TF edges in SST gradients and can produce clean results in noisy images because of its high filter weight (Kim and Ro, 2000).

2.2.3 Empirical orthogonal function (EOF) analysis

EOF analysis can describe temporal and spatial variations effectively and simultaneously and was used to describe SSTs and TFs in this study. Gradient values from the SEDM were processed in the EOF analysis of TFs.

$$F(x,t) = \sum_{i=1}^{n} e_i(x) c_i(t)$$

3. RESULTS AND DISCUSSION

3.1 Temporal and spatial variations in SSTs

3.1.1 SST variations by harmonic analysis

Harmonic analysis revealed that the mean SST was 10~25°C; SSTs generally decreased as latitude increased (Fig. 3). Annual amplitudes ranged from 4~11°C and varied by area. Area values, from highest to lowest, were as follows: WS (9~11°C), NES (8~9°C), SES (6~8°C), SS (6~7°C), and ECS (4~7°C), as shown in Fig. 4. The lowest amplitudes occurred in the ECS, which is affected by the Kuroshio Current (KC). The SS and SES are affected by the Tsushima Warm Current (TWC), a branch of the KC, and also showed low values. Higher amplitudes close to the continents characterized the WS and NES. Heat exchange at the continent exceeds that in the ocean (Yoon, 2001). to the SES, which maintains a relatively high SST.

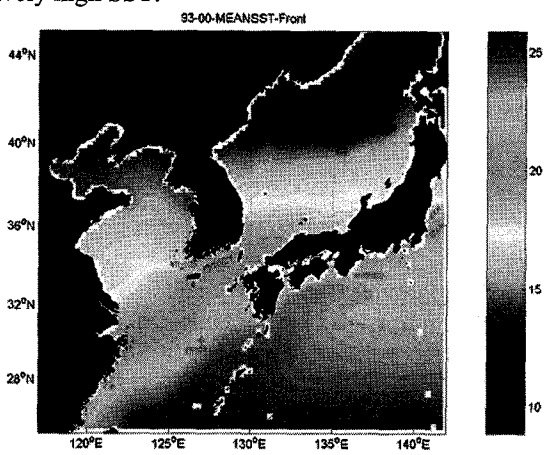

Fig. 3. Distributions of mean SSTs (℃) by harmonic analysis and Thermal Fronts (red dotted line).

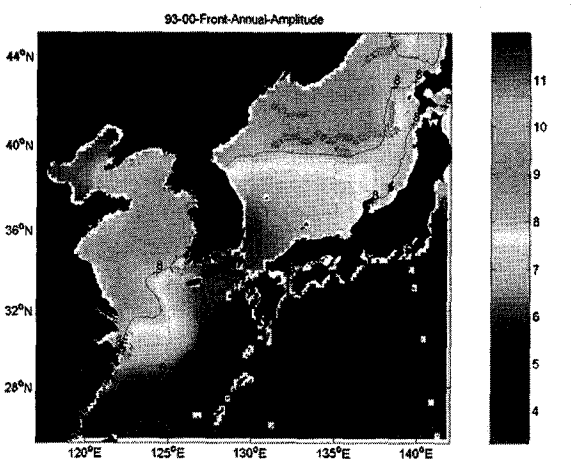

Fig. 4. Distributions of annual amplitudes (℃) by harmonic analysis and Thermal Fronts (red dotted line).

Annual phases at 210~240° (August) and 210~235° in the ECS reflected KC influences. The maximum SST

in the ECS was the earliest, at 210° (1 August) in all areas and was partly delayed at 235° (25 August). The WS phase ranged from 210~230° (25~30 August). The SES and NES division started at Ulleung Island and moved northeast; the phase in the SES occurred at 225~235° (15~20 August) in contrast to 235~240° (25~30 August) in the NES (Fig. 5). Semi-annual amplitudes showed overall small values so its effectiveness seemed to be low (Fig. 6).

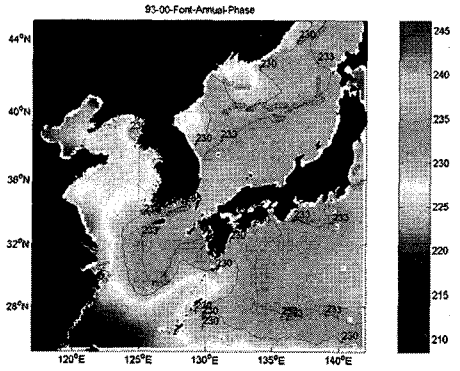

Fig. 5. Distributions of annual phases (°) by harmonic analysis and Thermal Fronts (red dotted line).

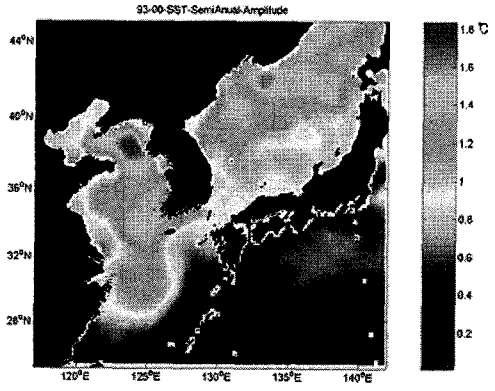

Fig. 6. Distributions of semi-annual amplitude (℃) by harmonic analysis.

3.1.2 SST variations by EOF analysis

EOF analysis revealed temporal and spatial aspects of SST variations in the Korean seas. First- and second-mode variances were 97.46% and 1.54%, respectively. The spatial components of the first mode showed higher variations close to the continent (Fig. 7a), similar to the annual amplitudes found by harmonic analysis. The temporal components showed annual variations with positive peaks in summer and negative peaks in winter (Fig. 7b). The results of power spectrum density (PSD) analysis of the temporal components showed that the first mode had a period of 1 year and the second mode had a period of 1 year or 6 months. Neither of these values matches the 3-year period of the El Niño event (Figs. 7c).

3.2 Distributions of thermal fronts

3.2.1 Thermal-front distributions determined by SEDM

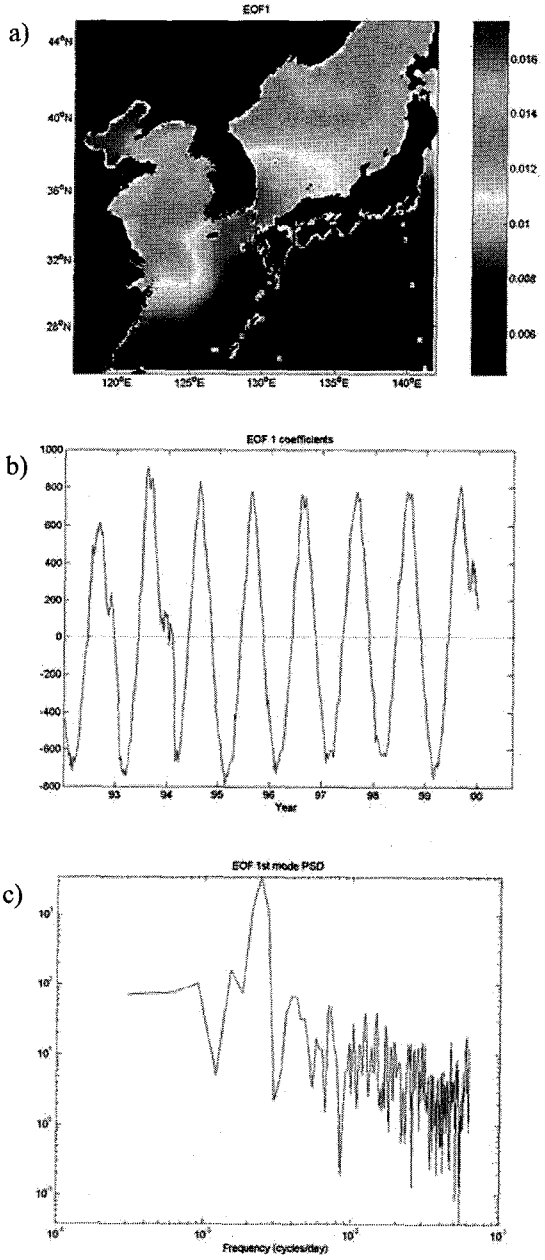

Fig. 7. a) spatial components, b) temporal components and c) PSDof temporal components in the first mode of SST gradients.

The pixels above threshold 0.3℃ were chosen TFs regions through processing of the sobel edge detection method. Only relatively distinct TFs were extracted using mean SSTs over wide areas, overall North East Asia Seas, rather than Korea coastal areas so the threshold value, 0.3℃, were most adequate with reference to previous researches (Fig. 9). Four different fronts were characterized. The Subpolar Front (SPF), an open sea front, ranged from 39°~40°N, 130°~140°E and divided the SES and NES. The Kuroshio Front (KF), a continental shelf front, formed between 28°~32°N, 124°~126°E within the ECS. The South Sea Coastal Front (SSCF) formed near the south coast (34°N,

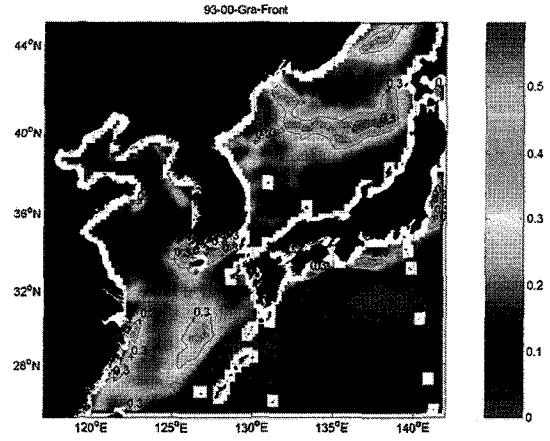

Fig. 9. Distributions of SST gradient values (℃) and Thermal Fronts (red dotted line).

a)

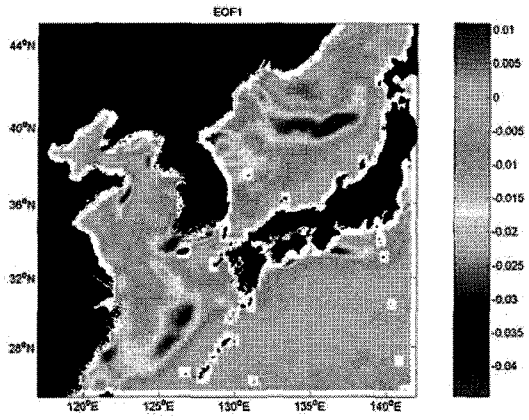

b)

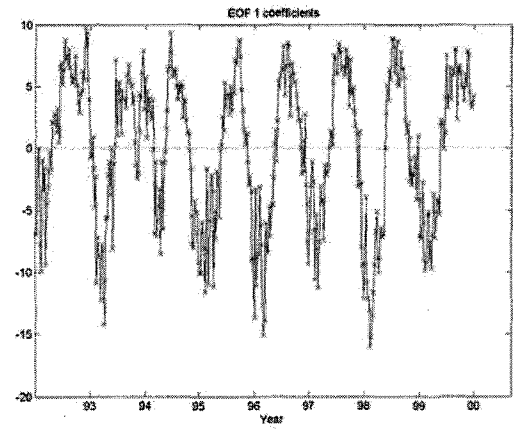

c)

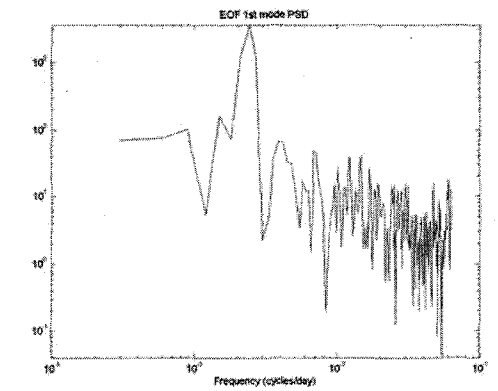

Fig. 10. a) spatial components, b) temporal components and c) PSD of temporal components in the first mode of SST gradients.

125°~129°E) within the SS. Finally, no distinct front was detected within the WS, although a tidal front did form.

3.2.2 EOF analysis of thermal fronts

An EOF analysis of TFs allowed a quantitative study of temporal variations. Variances explained by first-, second-, and third-mode analyses were 64.55%, 22.86%, and 12.58%, respectively. SPF, KF, and SSCF had striking negative values in the spatial components of the first mode, and the temporal components had a negative peak in March with annual variations (Figs. 10a, b). SPF and SSCF had negative values, but KF had positive spatial-component values in the second mode. In March and October. Power spectrum density (PSD) results for the temporal components had first- and second-mode periods of 1 year; the third mode showed a period of 6 months (Figs. 10c). SPF and SSCF had March and October peaks; KF had March and May peaks. We can't find marked peaks of TDF in the West Sea because it showed weak values.

3.2.3 Distribution analysis of SSTs and thermal fronts

All of the TFs in the Korean seas represented areas that divide regions of different annual amplitudes and phases. The SPF, KF and SSCF corresponded to borders dividing various annual amplitudes and phases. TFs were located on steep continental slopes; the SPF was found where the 3000-m deep continental shelf slopes up to the 1000~2000-m isobath; KF was located over a shallow continental shelf slope from the 500~1000-m isobath; and the SSCF was found over isobaths ranging from 20~100 m (Fig. 11). TDF cannot be recognized the location definitely because the spatial resolution of SST gradient images were not as high as its small scale, but it roughly seemed to be located in relatively steep isobath. The bottom bathymetry seemed to affect displacements of TFs and to influence seasonal variations. Also other researches issued that most of TFs occurred in sharp slope areas (Chiswell, 1994; Ullman and Cornillon, 2001).

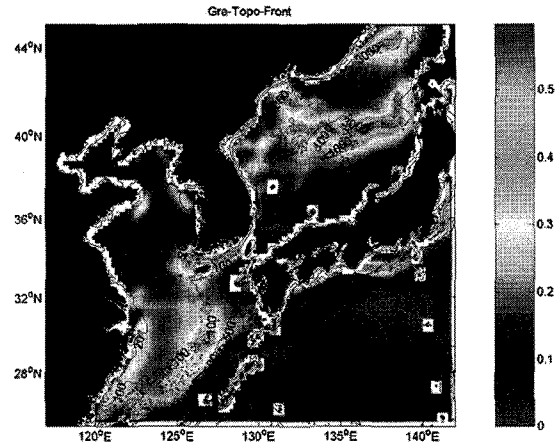

Fig. 11. Distributions of bottom bathymetry and Thermal Fronts (red dotted line) in SST gradient image.

4. CONCLUSION

Sea surface temperatures (SSTs) and thermal fronts (TFs) in the Korean seas were analyzed temporally and spatially using NOAA/AVHRR MCSST data for the 8-year period from 1993 to 2000. The results of harmonic analysis showed mean SST distributions of 10~25°C. SSTs generally decreased as latitude increased. Annual amplitudes and phases ranged from 4~11°C and 210~240°, respectively. By area, the highest to lowest amplitudes were as follows: the West Sea (9~11°C), the Northern East Sea (8~9°C), the Southern East Sea (6~8°C), the South Sea (6~7°C), and the East China Sea (4~7°C). Phases, from highest to lowest by area, showed the reverse order: the South Sea, 238~242°; the Southern East Sea, 235~240°; the Northern East Sea, 225~235°; the West Sea, 220~230°; and the East China Sea, 210~235°. With the exception of the East China Sea, which is influenced by the Kuroshio Current, areas with high amplitudes (large variations in SSTs) showed "low phases" (early maximum SST), while areas with low amplitudes (small variations in SSTs) had "high phases" (late maximum SST).

EOF analysis revealed temporal and spatial variations in SSTs in the Korean seas. The first mode reproduced 97.6% of the SST variance in the study area. This mode showed annual variations, with larger variations close to the coast. The variance of the second mode was unremarkable, reproducing 1.54% of the variance and representing no conspicuous phenomena. Temporal components from 1993 to 1995, during an El Niño event, exceeded those in other years, suggesting that El Niño does affect the Korean seas.

The Sobel edge detection method revealed four TFs: the Subpolar Front in the East Sea, the Kuroshio Front in the East China Sea, the South Sea Coastal Front in the South Sea, and a tidal front in the West Sea. TFs in the Korean seas included each type of ocean front classified by Yanagi (1987). This is therefore a good area to study ocean fronts. TF locations were similar to those of borders dividing differences in annual amplitudes and phases; such locations will influence seasonal variations. Furthermore, TFs occurred above areas of steep bathymetry. EOF analysis revealed temporal and spatial variations in TFs. The first, second, and third modes explained 64.55, 22.86, and 12.58% of variance, respectively. The SPF and SSCF were most significant in March and October, whereas the KF was most significant in March and May. This paper presented quantitative temporal and spatial distributions in SSTs from harmonic and EOF analyses based on satellite data. The analyses revealed TF distributions. We further think this research can contribute to advance researches about physical and chemical characteristics and variations of ocean fronts using ocean color data e.g. chlorophyll, suspended solids, physical data e.g. sea surface height, sea level anomaly, observed by satellite and to fisheries by helping fishing banks site estimation liking with locations of ocean fronts.

Acknowledgements

This study was supported by Dokdo Research Center project of Korea Ocean Research & Development Institute and Brain Korea 21 Project in 2006.

References

Berkin, I. and Cornillon, P., 2003, SST fronts of the pacific coastal marginal seas, *J. of Physical Oceanography*, 1(2):90~113.

Cayula, J. F. and Cornillon, P., 1995, Multi-Image edge detection for SST images, *J. of Atmospheric and Oceanic Technology*, 12:821-829.

Choi. Y. K., Shin M. S. and Lee B. G., 2000, Seasonal variations of temperature and salinity in Incheon coastal area, *J. of the Korean Environmental Sciences Society*, 9(2):131-136.

Deacon, G. E. R., 1982. Physical and biologicial zonation in the Southern Ocean. *Deep-Sea Research*, 29(1A): 1– 15.

Kim, E. and Ro, Y. J. 2000, Improved Method in estimating Ocean Current Vectors from Sequential Satellite Imageries, *J. Korean Soc. of Remote Sensing*, 16(3):199-209.

Lee, C. I., Cho, K. D. and Choi, Y. K., 2003, Spatial variation of the Polar Front in relation to the Tsushima Warm Current in the East Sea, *J. of Environmental Sciences*, 12(9):943-948.

McClain, E. P., W. G. Pichel, and C. C. Walton, 1985, Comparative Performance of AVHRR-Based Multichannel Sea Surface Temperatures, *Journal of Geophysical Research*, 90:11587-11601.

Mavor, T. P. and Bisagni, J. J., 2001, Seasonal variability of sea-surface temperature fronts on Georges Bank, *Deep-Sea Research*, 48:215-243.

Miller, P., 2004. Multi-spectral front maps for automatic detection of ocean colour features from SeaWiFS, *INT. J. of Remote Sensing*, 25(7-8):1437-1442.

Park, K. A. 2003, Seasonal Cycle of Sea Surface Temperature in the East Sea and its Dependence on Wind and Sea Ice, *proceedings of ACRS 2003 ISRS*, Vol. 2, pp. 1074-1076.

Wang, D., Liu, Y., Qi, Y. and Shi, P., 2001, Seasonal variability of thermal fronts in the Northern South China Sea from satellite data, *Geophysical Research Letters*, 28(20): 3963-3966.

Yoon, H. J., 2001. On Climatic Characteristics in the East Asian Seas by satellite data(NOAA, Topex/Poseidon), *Journal of the Korean Envion. Sci. Soc.*, 10(6): 423-429.